Scientific Research Publishing

American Journal of Analytical Chemistry, 2018, 9, 257-271
http://www.scirp.org/journal/ajac
ISSN Online: 2156-8278
ISSN Print: 2156-8251

Experimental Investigation and Modeling of Activity Coefficient at Infinite Dilution of Solutes Using Dicationic Solvent Based on Pyrrolidinium as a New Stationary Phase in Gas Chromatography

Ali Yahyaee[1*], Mina Nazifi[2], Mohsen Kianpour[3], Kurosh Tabar Heidar[2]

[1]School of Mechanical Engineering, Iran University of Science and Technology (IUST), Tehran, Iran
[2]Chemistry and Chemical Engineering Research Center of Iran, Tehran, Iran
[3]Iranian Catalyst Development (ICD), Tehran, Iran
Email: *Alidyahyaee@gmail.com

How to cite this paper: Yahyaee, A., Nazifi, M., Kianpour, M. and Heidar, K.T. (2018) Experimental Investigation and Modeling of Activity Coefficient at Infinite Dilution of Solutes Using Dicationic Solvent Based on Pyrrolidinium as a New Stationary Phase in Gas Chromatography. *American Journal of Analytical Chemistry*, **9**, 257-271.
https://doi.org/10.4236/ajac.2018.94020

Received: January 22, 2018
Accepted: April 23, 2018
Published: April 26, 2018

Abstract

Activity coefficients at infinite dilution, $\gamma^{\infty} i$, were calculated for 12 solutes, with organic solutes including linear alcohols (methanol, ethanol, propanol), linear alkanes (heptane, octane), benzene, toluene, cyclohexane, 1, 2-dichloroethane, trichloroethylene, acetonitrile and carbon tetrachloride. The values of $\gamma^{\infty} i$ were determined via either thermodynamic or artificial neural network modelling at different temperatures. A comparison between extracted results from these two methods confirmed that experimental and predicted results are roughly the same. The accuracy of predicted results proves this model is fully compatible with a wide range of solutes, and it can readily be used as an alternative to conventional gas-liquid chromatography for the measurements of activity coefficient at infinite dilution.

Keywords

Gas Chromatography, Ionic Liquid, Activity Coefficients at Infinite Dilution, Artificial Neural Network (ANN), Thermodynamic Modeling

1. Introduction

The measurements of activity coefficient at infinite dilution (γ^{∞}) are crucially important for either theoretical or practicing chemistry. This parameter describes the behavior of a solute completely surrounded by solvent molecules. Ac-

tivity coefficients at infinite dilution have been widely used for determining quantity of solutes' volatility and also made information about intermolecular energy between solvent and solute [1] [2] [3] [4] [5]. Values of γ^{∞} are decisive factors for the calculation of limiting separation factors necessary for the reliable design of distillation processes and the selection of solvents for extraction and extractive distillation. Moreover, activity coefficients are important for characterizing the behavior of liquid mixtures, predicting the existence of azeotrope, estimation of mutual solubility and calculation of Henry constants and partition coefficients.

Several methods were developed for the measurement of γ^{∞} such as dilutor technique (DT) [6] [7], inert gas stripping [6], differential ebulliometry [8], head space [9] and dew point techniques [10]. However, there are some drawbacks, in terms of time, cost and material, associated with each method. As chromatographic technique needs less than 1 gram of ILs and it can be considered as a cost-efficient, rapid and reliable method.

It is important to have a simple method to estimate all property distributions from known bulk properties. Artificial Neural Networks (ANN) has been widely applied to an extensive range of chemical engineering such as process modeling, optimization and PVT behavior over the last 20 years. In the mathematical algorithm of ANN, it is possible to relate input and output parameters without requiring prior knowledge of relationships between the process parameters [11] [12] [13] [14] [15].

In this work, values of γ^{∞} (the activity coefficients at infinite dilution) for 12 compounds in the following di-cationic ionic liquid with three phase loadings (10%, 15% and 20%) have been determined at various temperatures 308, 313, 318 and 323 K. Regarding the importance of activity coefficient at infinite dilution in thermodynamic and separation processes, a growing need for gaining activity coefficient in a simple and fast way has been felt. Therefore, an artificial neural network (ANN) model has been developed to predict the measures of γ^{∞} for an extensive range of solutes.

2. Experimental

2.1. Solvents and Solutes

All solvents were distilled from standard drying agents before use. All used Ionic Liquids were synthesized in CCERI [1]. N-Methyl pyrrolidine, 1, 9-di-bromononane, Lithium bis (trifluoromethylsulfonyl) imide and pentaoxide phosphor were purchased from Sigma-Aldrich company. 1 H NMR spectra (500 MHz) were recorded in deuterated ACN. Since the GLC process separated the solutes from any impurities, the solutes were used without further purification.

Structures of di-cationic ionic liquids $C_{12}(mPy)_2(NTf_2)_2$ is shown in **Figure 1**.

All solutes including linear alcohols (methanol, ethanol, propanol), linear alkanes (heptane, octane), benzene, toluene, cyclohexane, 1, 2-dichloroethane, trichloroethylene, acetonitrile and carbon tetra chloride, were supplied from MERCK.

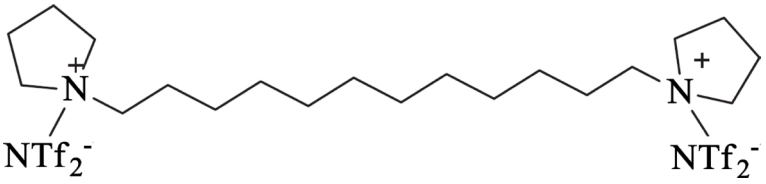

Figure 1. Structures of di-cationic ionic liquids C_{12} $(mPy)_2(NTf_2)_2$.

2.2. Analysis Method

Gas chromatography experiments were performed using a Varian CP-3800 gas chromatograph equipped with a heated 1041 injector and a thermal conductivity detector (TCD). The injector and detector temperatures were kept constant at 473 K during all experiments. The flow rate of helium was adjusted to obtain adequate retention times. The dead time was determined by injection of air with each solute. A personal computer equipped software as used for recording detector signals and corresponding chromatograms were obtained by Galaxie software.

2.3. Stationary Phase Preparation and Sample Injection Condition

Column packing, containing from 10%, 15% and 20% of stationary phase (IL) on Chromosorb W-AW (80 - 100 mesh), was prepared using the rotary evaporator technique. After evaporation of the dichloromethane under vacuum, the support was equilibrated at 323 K for 18 hours. The solid support material with the stationary phase was filled in a stainless steel column with an inner diameter of 3 mm and a length of 1 m. The weight of the packing material was calculated from the weights of the packed and empty column. A volume of the headspace vapor of samples of 0.1 - 0.5 micro liter was introduced to be in infinite dilution conditions. No differences in retention times t_r were found by injecting individual pure components or their mixtures. The measurements were carried out at temperatures between 308 and 323 K. At a given temperature, each experiment was repeated at least three times to verify the reproducibility. The difference of the retention times of the three measurements was ordinarily reproducible within (0.01 to 0.1) min.

Under aforementioned condition, the retention data for 12 solutes in 3 gas-chromatography columns with different phase load (10%, 15%, and 20%) and in different temperature (308, 313, and 318 K) have been obtained and used for calculating of activity coefficients at infinite dilution.

3. Modeling

3.1. Thermodynamic Modeling

Equation (1) suggested by Everett and Cruickshank *et al.* [16] [17] shown below, was used for determining of γ_i^{∞} values for the solute eluting in a carrier gas.

$$Ln\gamma_i^{\infty} = Ln\left(\frac{nRT}{V^n P^s}\right) - P^s \frac{B^{11} - V^s}{RT} + \frac{2B^{12} - V_{\infty}}{RT} JP^o \quad (1)$$

where n is the mole number of the stationary phase component inside the column, R is the ideal gas constant, T is the temperature of the oven, V^N is the standardized retention volume of the solute, P^o is the column outlet pressure (equal to atmospheric pressure), V^S the saturated liquid molar volume of the solute at T and V^∞ is the partial molar volume of the solute at infinite dilution in the solvent. B^{11} the second Virial coefficient of the solute in the gaseous state at temperature T, B^{12} the mutual Virial coefficient between the solute 1 and the carrier gas helium 2 and P^S is the probe vapor pressure at temperature T. The second and third terms in Equation (1) are correction terms that result from the non-ideality of the mobile gaseous phase. The molar volume of the solute V^S was determined from experimental densities, and the partial molar volumes of the solutes at infinite dilution V^∞ were assumed to be equal to V^S. The vapor pressure values were calculated using the Antoine equation [18] [19]. The standardized retention volume, V^N, can be calculated with the following relationship:

$$V_N = JU_o t_r' \tag{2}$$

The adjusted retention time, t_r' calculated from the difference between the retention times of a solute and that of air. U_0, the flow rate of the carrier gas, measured at the room temperature. The factor J corrects for the influence of the pressure drop along the column. Among of J relies on the pressure at the column outlet and inlet. This factor is defined by Equation (3).

$$J = \frac{3}{2}\frac{\left(p_i - p_o\right)^2 - 1}{\left(p_i - p_o\right)^3 - 1} \tag{3}$$

The values of B^{11} and B^{12} were calculated using the McGlashan and Potter [20].

The critical properties of the pure component (T_c^{11} and V_c^{11}) was extracted from the literature [21] [22] and the mutual critical data T_c^{12}, V_c^{12} were calculated using the combining rule presented by Hudson and McCoubrey [23].

Activity coefficients at infinite dilution of various types of solutes were computed in the di-cationic stationary phase with different phase load (10%, 15%, and 20%) in four temperatures (308, 313, 318, and 323 K). The obtained results of activity coefficients at infinite dilution for 12 solutes are presented in **Table 1**.

3.2. Artificial Intelligent Modeling

An artificial neural network was applied to model the system in order to predict activity coefficient of dilute solution for lots of chemical compounds. 144 data sets were used for training and testing. 70% of these data have been used for training, test data and validate data used the equal percentage of 15.

One of the most popular and commonly used networks is the multilayer perceptron network (MLP). The MLP configuration has gained a widespread use in static regression applications [24]-[29]. It can have one or more hidden layer(s).Whereas Cybenko [30] and Huang *et al.* [31] had proved that a one hidden layer network is suitable to represent any type of multidimensional

Table 1. Activity coefficient of solutes at infinite dilute solution.

Solutes	T/K	10	15	20
Benzene	308	0.2653	0.3249	0.2644
	313	0.2778	0.3322	0.2597
	318	0.2751	0.4048	0.2744
	323	0.3020	0.4219	0.3101
Methanol	308	0.3905	0.4311	0.4185
	313	0.3656	0.4528	0.3859
	318	0.3571	0.4696	0.4092
	323	0.4426	0.5885	0.4454
Ethanol	308	0.4968	0.5988	0.5385
	313	0.4626	0.5990	0.4967
	318	0.4373	0.6220	0.5130
	323	0.5625	0.7060	0.5372
Propanol	308	0.6000	0.7150	0.6612
	313	0.6142	0.7967	0.6564
	318	0.5975	0.6890	0.6201
	323	0.6716	0.8444	0.6473
Acetonitrile	308	0.1529	0.1838	0.1596
	313	0.1594	0.1968	0.1565
	318	0.1620	0.2021	0.1591
	323	0.1991	0.2310	0.1796
Cyclohexane	308	2.4003	2.6037	2.3272
	313	2.3132	2.7101	2.2169
	318	2.2900	2.7948	2.2222
	323	2.3168	3.9487	2.4903
Toluene	308	0.3538	0.4473	0.3446
	313	0.3732	0.4436	0.3468
	318	0.3726	0.4538	0.3705
	323	0.3753	0.4306	0.4171
Heptane	308	4.5788	5.5034	5.0667
	313	5.3570	5.5809	4.7640
	318	4.6549	5.5048	4.8457
	323	5.7666	5.8925	5.6490
Octane	308	7.0796	7.9705	7.6836
	313	5.9958	7.4999	6.6670
	318	5.7462	7.3969	6.8222
	323	6.3740	9.2261	9.1810
Dichloroethane	308	0.1622	0.2034	0.1712
	313	0.2052	0.2481	0.1670
	318	0.2362	0.2919	0.1976
	323	0.3322	0.4202	0.2465
Carbontetrachloride	308	0.4863	0.5602	0.4735

Continued

	313	0.5864	0.6787	0.4642
	318	0.7309	0.8205	0.5208
	323	0.8610	1.1592	0.6568
Trichloroethylene	308	0.2722	0.3176	0.2680
	313	0.3210	0.3880	0.2615
	318	0.3823	0.4747	0.2560
	323	0.5137	0.6638	0.3002

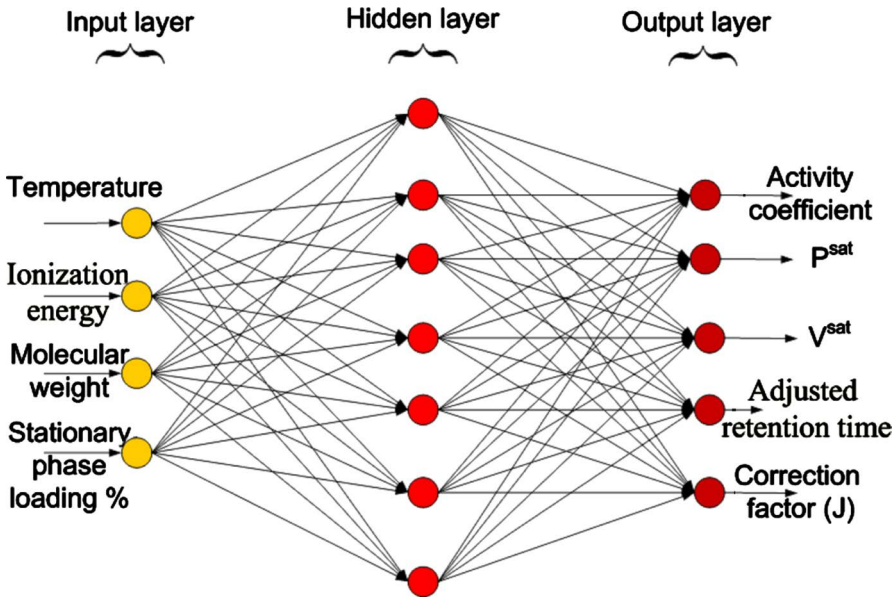

Figure 2. The selected structure for the artificial neural network (Ann).

non-linear function with sufficient number of neurons and more hidden layers may result in over-fitting, therefore, in this work, one hidden layer was applied as displayed in **Figure 2**. In addition, a procedure modified at our last works [32] [33] was selected to design a relatively small and entirely accurate network. The procedure flowchart is shown in **Figure 3**. At the first step of the procedure, a training method was randomly applied to find the number of neurons in the hidden layer that minimizes the mean squared normalized error (MSE) (defined by Equation (4)) of the network.

$$\mathrm{MSE} = \frac{1}{N}\sum_{i=1}^{N} e_i^2 \tag{4}$$

where e_i is the differences between experimental and predicted data.

In order to improve the model generalization and prevent over-fitting, the number of neurons has to be chosen so that the number of internal parameters in the network does not exceed the number of training data sets [34]. The number of internal parameters was calculated according to the following equation [35]:

$$n_{tot} = \left(n_i + 1\right) \times n_{h1} + \left(n_{h1} + 1\right) \times n_{h2} + \cdots + \left(n_{hn} + 1\right) \times n_o \tag{5}$$

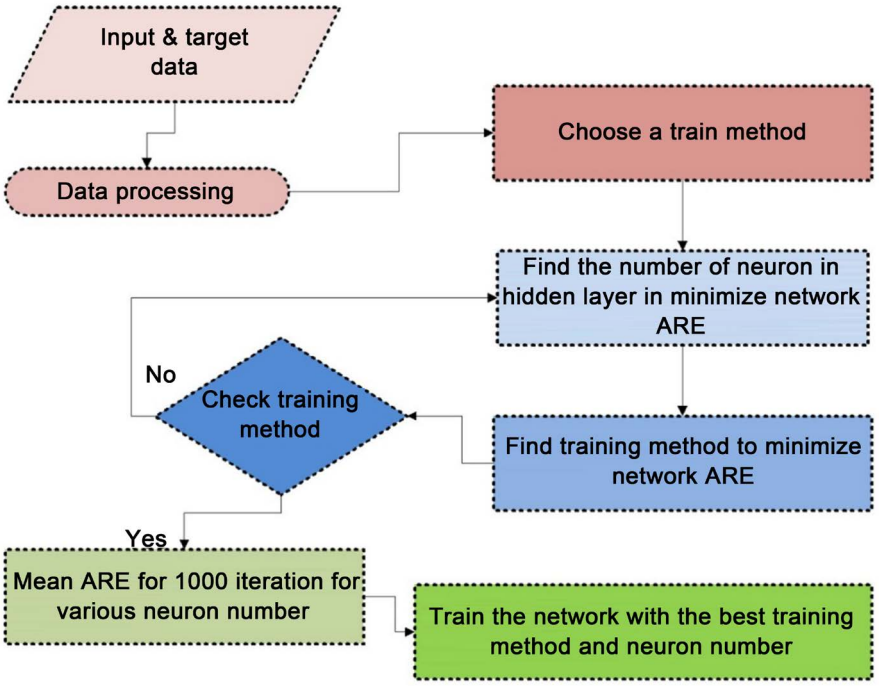

Figure 3. The procedure to design artificial neural network.

where, n_{tot} is the total number of network parameters, n_o is the number of outputs and n_{hi} is the number of the neurons in the ith hidden layer. In this work, the maximum number of neurons that can be used in hidden layer in this system to prevent over-fitting was calculated to be seven. Thus, the choice of neuron number was limited in the range of 1 - 7 neurons for the hidden layer. At the second step, the network with the neuron number of the last step was used to find a training method that leads to minimum MSE of the network. If the network MSE was less than the desirable MSE the third step was started. Otherwise, the last two steps were repeated till the desirable MSE value was reached.

The applied training methods consist of Bayesian Regularization (BR), BFGS[1] Quasi-Newton (BFG), Resilient Backpropagation (RP), Scaled Conjugate Gradient (SCG), Conjugate Gradient with Powell/Beale Restarts (CGB), Levenberg-Marquardt (LM), Fletcher-Powell Conjugate Gradient (CGF), Polak-Ribiére Conjugate Gradient (CGP), One Step Secant (OSS), Variable Learning Rate Gradient Descent (GDX), Gradient Descent with Momentum (GDM), and Gradient Descent (GD).

At the third step, the selected training method was applied to train the network using a number of neurons (1 - 8). Each of these trainings was repeated 1000 time and the means of MSEs for the repeated trainings were recorded.

In addition to MSE, correlation coefficients (R) are commonly used to verify ANN models. In this work R has also been applied as defined by Equation (6).

$$R = \frac{\sum(\alpha_i - \bar{\alpha})(\tau_i - \bar{\tau})}{\sqrt{\sum(\alpha_i - \bar{\alpha})^2 \sum(\tau_i - \bar{\tau})^2}} \tag{6}$$

[1]Hesian updating methods of Broyden, Fletcher, Goldfarb, Shanno (BFGS).

where, τ_i is the target and α_i is the network output and $\overline{\tau}, \overline{\alpha}$ are the mean amount of the data.

4. Results

The ANN model was also employed to predict activity coefficient at infinite dilution of different solutes. The procedure described in section 3 was applied to design the model. Temperature, Ionization energy, Molecular weight and stationary phase loading were chosen as the input data of network and Activity coefficient, Saturated pressure, Saturated volume, Adjusted retention time and the correction factor (J) were chosen as the output data.

Levenberg-Marquardt (LM) method was found to have the minimum error as shown in Table 2. Mean squared normalized error of the ANN model is indicated in Figure 4. This figure shows that using seven neurons has resulted in a minimum error. Therefore, this structure (144:7:1) was selected as the best network to model this system. Hence, a network with seven neurons in the hidden layer which trained by Levenberg-Marquardt (LM) method, selected as the best network. Optimal network structure can be seen in Figure 2. This network consists of 144 input data that divided to train, test and validation data.

The results of ANN model and experimental data are depicted in Figure 5 and Figure 6. Figure 5, the regression plot of the ANN model and experimental data, shows an accurate prediction for the model. The error histogram with twenty

Table 2. The results of different training methods; Mean squared normalized error of the data.

	Overall data	Train data	Validate data	Test data
Trainb	1714.857	1752.72	1070.62	2186.99
trainbfg	63.4526	50.5515	63.4818	122.065
Trainbr	16.33893	16.3389	1450277	2450.28
Trainc	572.8554	571.264	793.043	359.9
traincgb	297.3109	277.746	368.5	315.055
traincgf	283.4068	276.4	279.52	319.142
traincgp	270.6267	213.914	391.736	407.301
Traingd	270.6267	261.347	350.299	233.134
traingda	270.6267	266.085	159.743	402.153
traingdm	270.6267	298.904	215.837	196.885
Traingd	270.6267	282.871	165.608	319.99
Trainlm	0.111587	0.08726	0.16761	0.16613
trainoss	26.00845	28.9234	25.3603	13.4069
Trainr	162.3016	177.837	172.875	81.1113
Trainrp	80.94391	87.1408	73.3158	60.4043
Trains	71.17467	74.2786	65.688	62.5527
trainscg	71.17467	76.5718	54.7914	63.0255

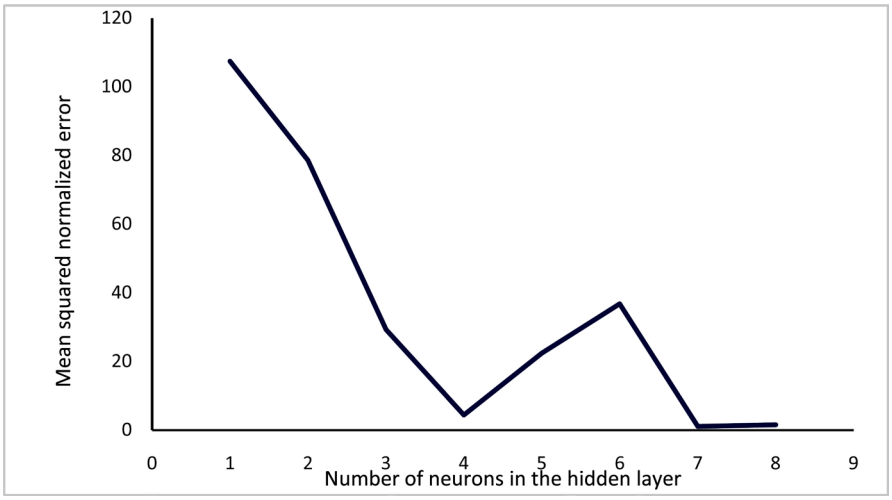

Figure 4. The variation of average relative error and R with number of neurons in the hidden layer.

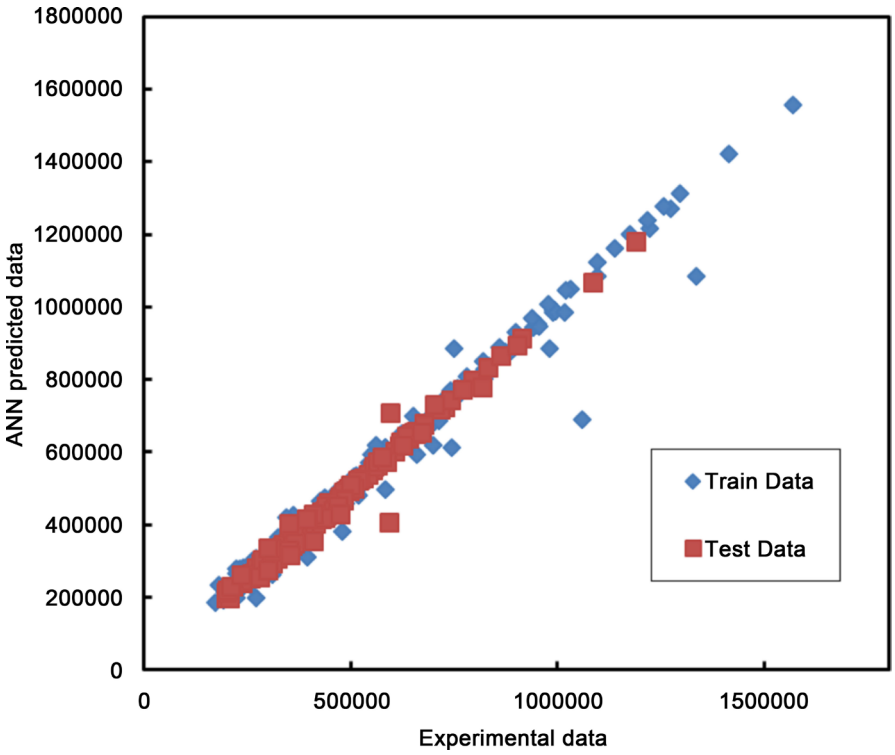

Figure 5. Comparing of the experimental data and predicted results of network.

bins is shown in Figure 6. According to the Figure 6, it can be seen that the histogram has a peak around 0.017. Table 3 reports the errors for training and test stages of the ANN model. The weight and biases of this network were reported in Table 4 in order to predict resulted data, and also use this model for finding directly the precise amount of activity coefficients of other materials without carrying out time consuming experiments and using thermodynamic modeling.

In this work, having calculated the activity coefficients at infinite dilution in three different ways, a comparison between their final results has been drawn.

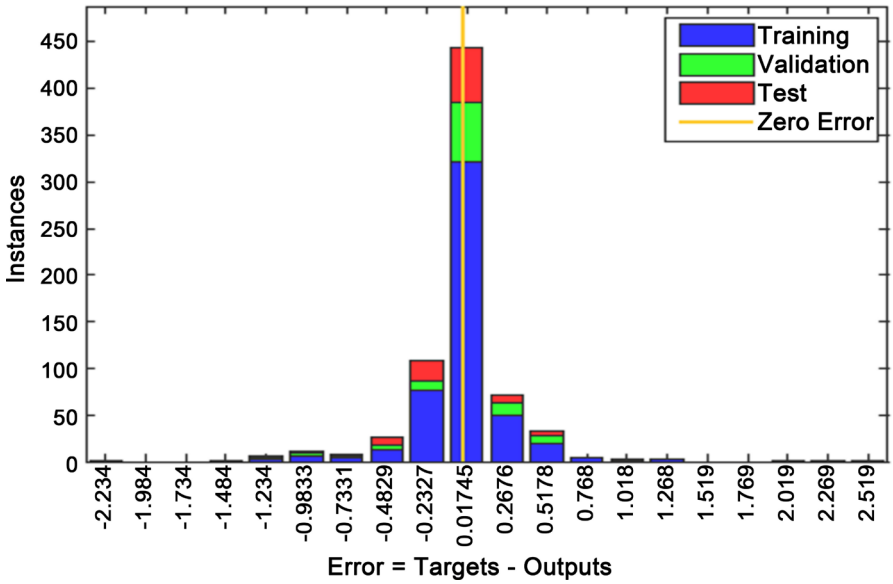

Figure 6. Error histogram with 20 bins obtained using the presented model and number of pure compounds in each range.

Table 3. Statistical properties of trained ANN.

Data	Number	average relative error percent	R
Train	102	0.0873	0.994
Validate	21	0.1676	0.988
Test	21	0.1676	0.988
Overall	144	0.1116	0.993

Table 4. Weights and Biases of the selected artificial neural network.

Hidden layer neuron	1	2	3	4	5	6	7
	Optimal neural network Output Weights						
Vsat	0.84599	−0.64791	0.041857	−6.46673	−0.74503	0.065056	−0.00501
Psat	−0.43605	−0.60363	−0.67509	1.42567	−2.02872	−0.56282	−1.36424
t'	−0.62664	3.026805	1.83053	4.555867	8.531572	2.544383	3.790702
J	−0.20605	0.29563	0.279518	0.150291	1.031618	0.327164	0.489746
Γ	1.07002	−1.57239	−0.27529	−8.62001	−1.16475	0.018138	−0.37616
	Optimal neural network Biases						
Bias	6.290099	−2.47087	−0.35334	0.533857	−0.31865	3.139325	−0.59779

The first method is based on using experimental data extracted from the thermodynamic model. In the second method, data were obtained from ANN model and the third method is based on the thermodynamic model used ANN predicted data. Table 5 presents the results achieved through these methods. In this comparison, the first method that used experimental data for calculating activity coefficient is chosen as the basis to calculate errors. As it is shown in Table 5, that predicted activity coefficient extracted from ANN model has the smallest error. The Average Overall error of test data for the second and third method is

Table 5. Comparison between activity coefficient of the test data that calculated with three different method; Using thermodynamic model that used experimental data; ANN output; Using thermodynamic model that used ANN prediction data.

Calculated test data using thermodynamic model	Output			
	Predicted gama using ANN	calculated by ANN data	error of the ANN predictions	error of the thermodynamic predictions by use of ANN outputs
0.302	0.23	0.4615	0.072	0.1595
2.3168	2.587	3.5023	0.2702	1.1855
0.3726	0.5664	0.3205	0.1938	0.0521
5.357	5.60408	12.638	0.24708	7.281
0.2362	0.2451	0.2613	0.0089	0.0251
0.4863	0.6772	1.079	0.1909	0.5927
0.5237	0.6686	0.3	0.1449	0.2237
0.4219	0.21254	0.70601	0.20936	0.28411
0.4311	0.351215	0.4143	0.079885	0.0168
2.7947	2.8557	9.1918	0.061	6.3971
0.4306	0.98219	0.40056	0.55159	0.03004
5.5809	6.06188	7.2775	0.48098	1.6966
5.8924	6.3578	7.92725	0.4654	2.03485
0.6637	0.6582	0.42118	0.0055	0.24252
0.4967	0.55293	0.36778	0.05623	0.12892
0.6564	0.836017	0.26141	0.179617	0.39499
2.3271	2.7655	0.8657	0.4384	1.4614
0.3704	0.515176	0.67011	0.144776	0.29971
7.6835	6.57	1.82817	1.1135	5.85533
0.17117	0.27	0.18824	0.0988	0.0818
0.24652	0.1968	0.28503	0.04972	0.03851
Average Overall error of test data			0.24113	1.353213

0.24 and 1.35, respectively.

5. Discussion

The chromatographic data has been used in order to determine the values of activity coefficients at infinite dilution by either thermodynamic or ANN model. In the thermodynamic model, the values of activity coefficients at infinite dilution have been calculated for 12 solutes at different temperatures (308, 313, 318 and 323 K) in three columns with different stationary phase loadings (10%, 15% and 20%). It can be seen that the results obtained from two models come from a broadly similar direction. As a result, ANN can be efficiently used to measure the values of activity coefficients at infinite dilution in different temperatures. A great advantage associated with ANN model is that the values of activity coefficients at infinite dilution can be directly obtained through retention time (t_r), the saturated liquid molar volume (V^s), the probe vapor pressure (P^s) and the ioni-

zation energy (I) at T, without getting involved in complicated thermodynamic computations. According to the strong similarity between the results of two models, the range of solutes can be expanded, and the values of activity coefficients at infinite dilution can be predicted precisely by ANN model for an extensive range of solutes according to their retention time (t_r), the saturated liquid molar volume (V^s), the probe vapor pressure (P^s) and the ionization energy (I) at the wanted temperature (T). As in ANN model all the steps related to the calculation of physiochemical parameters can be skipped, ANN model can be considered as a time-saving and cost-efficient technique for determination of activity coefficients at infinite dilution, in comparison with the thermodynamic model. As it can be seen in **Table 1**, the Train error in ANN model is 0.087; Validate error is 0.167; Test error is 0.166 and the overall error is 0.111.

References

[1] Heintz, A., Kulikov, D.V. and Verevkin, S.P. (2001) Thermodynamic Properties of Mixtures Containing Ionic Liquids. 1. Activity Coefficients at Infinite Dilution of Alkanes, Alkenes, and Alkylbenzenes in 4-Methyl-n-Butylpyridinium Tetrafluoroborate Using Gas– Liquid Chromatography, Journal of Chemical & Engineering Data, 46 1526-1529. https://doi.org/10.1021/je0101348

[2] Heintz, A., Kulikov, D.V. and Verevkin, S.P. (2002) Thermodynamic Properties of Mixtures Containing Ionic Liquids. 2. Activity Coefficients at Infinite Dilution of Hydrocarbons and Polar Solutes in 1-Methyl-3-Ethyl-Imidazolium bis (Trifluoromethyl-Sulfonyl) Amide and in 1, 2-Dimethyl-3-Ethyl-Imidazolium bis (Trifluoromethyl-Sulfonyl) Amide Using Gas-Liquid Chromatography. *Journal of Chemical & Engineering Data*, **47**, 894-899. https://doi.org/10.1021/je0103115

[3] Heintz, A., Kulikov, D.V. and Verevkin, S.P. (2002) Thermodynamic Properties of Mixtures containing ionic liquids. Activity coefficients at Infinite Dilution of Polar Solutes in 4-Methyl-N-Butyl-Pyridinium Tetrafluoroborate Using Gas-Liquid Chromatography. *The Journal of Chemical Thermodynamics*, **34**, 1341-1347. https://doi.org/10.1006/jcht.2002.0961

[4] Cruickshank, A., Windsor, M. and Young, C. (1966) The Use of Gas-Liquid Chromatography to Determine Activity Coefficients and Second Virial Coefficients of Mixtures. I. Theory and Verification of Method of Data Analysis. *Proceedings of the Royal Society of London A*: *Mathematical*, *Physical and Engineering Sciences*, The Royal Society, 259-270.

[5] Dohnal, V. and Horáková, I. (1991) A New Variant of the Rayleigh Distillation Method for the Determination of Limiting Activity Coefficients. *Fluid Phase Equilibria*, **68**, 173-185. https://doi.org/10.1016/0378-3812(91)85016-N

[6] Lerol, J.-C., Masson, J.-C., Renon, H., Fabries, J.-F. and Sannier, H. (1977) Accurate Measurement of Activity Coefficient at Infinite Dilution by Inert Gas Stripping and Gas Chromatography. *Industrial & Engineering Chemistry Process Design and Development*, **16**, 139-144. https://doi.org/10.1021/i260061a609

[7] Belting, P.C., Rarey, J., Gmehling, J., Ceriani, R., Chiavone-Filho, O. and Meirelles, A.J. (2014) Measurements of Activity Coefficients at Infinite Dilution in Vegetable Oils and Capric Acid Using the Dilutor Technique. *Fluid Phase Equilibria*, **361**, 215-222. https://doi.org/10.1016/j.fluid.2013.10.035

[8] Eckert, C., Newman, B., Nicolaides, G. and Long, T. (1981) Measurement and Ap-

plication of Limiting Activity Coefficients. *AIChE Journal*, **27**, 33-40. https://doi.org/10.1002/aic.690270107

[9] Anand, S.C., Grolier, J.P.E., Kiyohara, O., Halpin, C.J. and Benson, G.C. (1975) Thermodynamic Properties of Some Cycloalkane-Cycloalkanol Systems at 298.15K. III. *Journal of Chemical & Engineering Data*, **20**, 184-189. https://doi.org/10.1021/je60065a020

[10] Trampe, D.B. and Eckert, C.A. (1993) A Dew Point Technique for Limiting Activity Coefficients in Nonionic Solutions. *AIChE Journal*, **39**, 1045-1050. https://doi.org/10.1002/aic.690390613

[11] Harrington, P. (1993) Transfer Functions in Artificial Neural Networks, Center for Intelligent Chemical Instrument. Department of Chemistry, Ohio University, Athens, OH.

[12] Werbos, P. (1974) Beyond Regression: New Tools for Prediction and Analysis in the Behavioral Sciences. PhD Thesis, Harvard University, Cambridge.

[13] Turan, N.G., Mesci, B. and Ozgonenel, O. (2011) Artificial Neural Network (ANN) Approach for Modeling Zn (II) Adsorption from Leachate Using a New Biosorbent. *Chemical Engineering Journal*, **173**, 98-105. https://doi.org/10.1016/j.cej.2011.07.042

[14] Astray, G., Morales, J., González-Temes, M., Mejuto, J.C. and Magdalena, A.J. (2015) Alternative Method to Predict Activity Coefficients at Infinite Dilution of Hydrocarbons in Aqueous Solutions. *Mediterranean Journal of Chemistry*, **3**, 1073-1082. https://doi.org/10.13171/mjc.3.6.2015.01.02.11.25.astray

[15] Behrooz, H.A. and Boozarjomehry, R.B. (2017) Prediction of Limiting Activity Coefficients for Binary Vapor-Liquid Equilibrium Using Neural Networks. *Fluid Phase Equilibria*, **433**, 174-183. https://doi.org/10.1016/j.fluid.2016.10.033

[16] Everett, D. (1965) Effect of Gas Imperfection on GLC Measurements: A Refined Method for Determining Activity Coefficients and Second Virial Coefficients. *Transactions of the Faraday Society*, **61**, 1637-1645. https://doi.org/10.1039/tf9656101637

[17] Cruickshank, A., Gainey, B., Hicks, C., Letcher, T., Moody, R. and Young, C. (1969) Gas-Liquid Chromatographic Determination of Cross-Term Second Virial Coefficients using Glycerol. Benzene + Nitrogen and Benzene + Carbon Dioxide at 50 C. *Transactions of the Faraday Society*, **65**, 1014-1031. https://doi.org/10.1039/TF9696501014

[18] Riddick, J.A., Bunger, W.B. and Sakano, T.K. (1986) Organic Solvents: Physical Properties and Methods of Purification. 4th Edition, Wiley Interscience, Hoboken.

[19] TRC (1990) Thermodynamic Tables. Thermodynamics Research Centre, The Texas A&M University System College Station, College Station.

[20] McGlashan, M.L. and Potter, D.J.B. (1951) An Apparatus for the Measurement of the Second Virial Coefficient using Glycerol. *Proceedings of the Royal Society*, **267**, 448-456.

[21] Reid, R.C., Prausnitz, J.M. and Sherwood, T.K. (1977) The Properties of Gases and Liquids. 3rd Edition, Chem. Eng. Series, McGraw-Hill, New York.

[22] Prausnitz, J.M., Lichtenthaler, R.N. and Azevedo, E.G. (1986) Molecular Thermodynamics of Fluid Phase Eqilibria. 2nd Edition, Prentice Hall, New York.

[23] Hudson, G.H. and McCoubrey, J.C. (1960) Intermolecular Forces between Unlike Molecules. A More Complete Form of the Combining Rules. *Transactions of the Faraday Society*, **56**, 761-766. https://doi.org/10.1039/tf9605600761

[24] Arriagada, J., Olausson, P. and Selimovic, A. (2002) Artificial Neural Network Simulator for SOFC Performance Prediction. *Journal of Power Sources*, **112**, 54-60. https://doi.org/10.1016/S0378-7753(02)00314-2

[25] Boccaletti, C., Cerri, G. and Seyedan, B. (2000) A Neural Network Simulator of a Gas Turbine with a Waste Heat Recovery Section. *Journal of Engineering for Gas Turbines and Power*, **123**, 371-376.

[26] Fast, M., Assadi, M. and De, S. (2009) Development and Multi-Utility of an ANN Model for an Industrial Gas Turbine. *Applied Energy*, **86**, 9-17. https://doi.org/10.1016/j.apenergy.2008.03.018

[27] Sadrzadeh, M., Mohammadi, T., Ivakpour, J. and Kasiri, N. (2009) Neural Network Modeling of Pb^{2+} Removal from Wastewater using Electrodialysis. *Chemical Engineering and Processing: Process Intensification*, **48**, 1371-1381. https://doi.org/10.1016/j.cep.2009.07.001

[28] Messikh, N., Bousba, S. and Bougdah, N. (2017) The Use of a Multilayer Perceptron (MLP) for Modelling the Phenol Removal by Emulsion Liquid Membrane. *Journal of Environmental Chemical Engineering*, **5**, 3483-3489.

[29] Shekofteh, Y., Almasganj, F. and Daliri, A. (2015) MLP-Based Isolated Phoneme Classification using Likelihood Features Extracted from Reconstructed Phase Space. *Engineering Applications of Artificial Intelligence*, **44**, 1-9. https://doi.org/10.1016/j.engappai.2015.05.001

[30] Cybenko, G. (1989) Approximation by Superpositions of a Sigmoidal Function. *Mathematics of Control, Signals, and Systems* (*MCSS*), **2**, 303-314. https://doi.org/10.1007/BF02551274

[31] Huang, G.-B., Chen, Y.-Q. and Babri, H.A. (2000) Classification Ability of Single Hidden Layer Feedforward Neural Networks. *IEEE Transactions on Neural Networks*, **11**, 799-801. https://doi.org/10.1109/72.846750

[32] Kianpour, M., Sobati, M.A. and Shahhosseini, S. (2012) Experimental and Modeling of CO_2 Capture by Dry Sodium Hydroxide Carbonation. *Chemical Engineering Research and Design*, **90**, 2041-2050. https://doi.org/10.1016/j.cherd.2012.04.005

[33] Tirandazi, B., Yahyaee, A., Kianpour, M. and Shahhosseini, S. (2017) Experimental Investigation and Modeling of Viscosity Effect on Carbon Dioxide Absorption using Sodium Hydroxide. *Journal of Environmental Chemical Engineering*, **5**, 2597-2604.

[34] Hush, D.R. and Horne, B.G. (1993) Progress in Supervised Neural Networks. *IEEE Signal Processing Magazine*, **10**, 8-39. https://doi.org/10.1109/79.180705

[35] Farshad, F., Iravaninia, M., Kasiri, N., Mohammadi, T. and Ivakpour, J. (2011) Separation of Toluene/n-Heptane Mixtures Experimental, Modeling and Optimization. *Chemical Engineering Journal*, **173**, 11-18.

Nomenclature

$\bar{\alpha}$	mean amount of the data	Equation (6)
a_i	network output	Equation (6)
B^{11}	the second virial coefficient	Equation (1)
B^{12}	the mutual virial coefficient	Equation (1)
γ_i^{∞}	activity coefficient at infinite dilution	Equation (1)
e_i	the differences between experimental and predicted data	Equation (4)
J	correction factor	Equations (1)-(3)
N	mole number of the stationary phase component inside the column	Equation (1)
n_0	number of outputs	Equation (5)
n_{tot}	total number of network parameters	Equation (5)
n_{hi}	number of the neurons in the ith hidden layer	Equation (5)
P_o	outlet pressure	Equations ((1), (3))
P_i	inlet pressure	Equation (3)
P^s	probe vapor pressure	Equation (1)
R	ideal gas constant	Equation (1)
R	correlation coefficient	Table 3
T	Temperature	Equation (1)
T_c^{11}	critical temperature	Equation (1)
T_c^{12}	mutual critical temperature	Equation (1)
t_r'	adjusted retention time	Equation (2)
τ_i	the target	Equation (6)
$\bar{\tau}$	mean amount of the data	Equation (6)
U_0	flow rate of carrier gas	Equation (2)
V^N	standardized retention volume	Equations ((1), (2))
V^s	molar volume of solute	Equation (1)
V^{∞}	partial molar volumes of the solutes at infinite dilution	Equation (1)
V_c^{11}	critical volume	Equation (1)
V_c^{12}	mutual critical volume	Equation (1)